ELSEVIER

Applied Acoustics 62 (2001) 411–428

applied acoustics

www.elsevier.com/locate/apacoust

Further assessment of the coupling load decomposition technique for the vibration analyses of planar coupled structures

L. Cheng *, M. Hatam

Laboratory of Vibro-Acoustics (LAVA), Mechanical Engineering Department, Laval University, PQ, Canada G1K 7P4

Received 1 August 1999; received in revised form 14 January 2000; accepted 3 February 2000

Abstract

Vibration analyses of various line-coupled structures are conducted in this paper using the newly developed Coupling Load Decomposition technique. Examples are given to illustrate how this approach may be used in practice. Various factors related to the practical application of the technique are investigated. The approach is applied to systems composed of a main plate as the master structure and different substructures. Plate-like structures and beam-stiffened plates are studied and the results are compared to finite element results. Applications to the case of periodic structures or systems with repeated substructures are also investigated. It is shown that the method is very efficient in such cases leading to satisfactory results in low and medium frequency ranges.

1. Introduction

Vibrations of mechanically coupled structures have been extensively investigated in the past few decades. One typical example is shown in Fig. 1, which is composed of a thin plate as the master structure to which several substructures are coupled. In addition to the commonly used finite element method, various simulation methods have been developed in the past. A summary of existing methods can be found in Ref. [1]. One can mention the statistical energy analysis [2], fuzzy structure theory [3], powerflow approach [4] as well as various methods dealing with particular configurations.

* Corresponding author now at Department of Mechanical Engineering, The Hong Kong Polytechnic University, Kowloon, Hong Kong. Tel.: +852 2766-6769; fax: +852 2365-4703.

E-mail address: mmlcheng@polyu.edu.hk

0003-682X/01/$ - see front matter
PII: S0003-682X(00)00031-1

In our previous work [1], a method, named Coupling Load Decomposition (CLD) technique was proposed to use substructure compliance functions in the study of forced vibrations of line-coupled structures. The technique permits the use of numerical, analytical and experimental data to characterize the substructure compliance functions. It can therefore be regarded as a hybrid method. Compliance functions which carry the dynamic information of substructures are easier to work with compared to the modal characteristics used in modal techniques [5,6]. For real-life complex substructures, the compliance data can be obtained experimentally. The technique does not require to determine the modal characteristics of substructures, in contrast to several existing methods. This presents a major advantage since modal identification is a more difficult task than compliance measurement or, even if it is possible, it may be difficult to work with computationally [7].

Several examples are given in this paper to numerically assess the technique. The configurations were chosen among line-coupled structures which are of practical interest and therefore frequently treated in the literature:(1) plate assemblies with sub-plates coupled in rotation along the junction;(2) ribbed plates involving both transversal and rotational coupling between the plate and the beams;(3) periodic structures or systems with repeated sub-structures.

Numerical results are restricted to low and middle frequency ranges, since a semi-analytical formulation is used to model the main structure. However, the proposed methodology is quite general and may be used in conjunction with any other energy

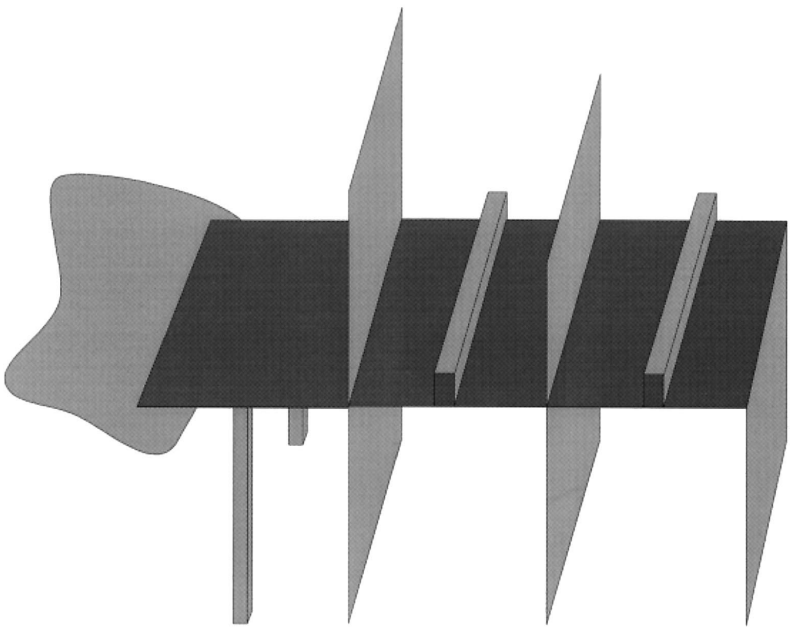

Fig. 1. An example of plate-like structures.

based formulations. Whenever possible, simulated results are compared to finite element simulations.

2. Modeling procedure

The modeling procedure is briefly summarized in this section. More details can be found in Ref.[1]. Consider a system composed of a thin rectangular plate as the master structure shown in Fig. 2, with $-b \leqslant x \leqslant b$, $-h \leqslant y \leqslant h$ and $-t \leqslant z \leqslant t$. The plate is supported by translational and rotational springs and the boundaries. Small deformations are assumed and, classical linear thin plate theory (Love–Kirchhoff) can be used.

The transverse displacement of the rectangular plate is approximated by a series:

$$w(x, y, t) = \sum_{i=0}^{m}\sum_{j=0}^{n} a_{ij}(t)\left(\frac{x}{b}\right)^{i}\left(\frac{y}{h}\right)^{j} \tag{1}$$

Using the Rayleigh–Ritz method, the coefficients of the polynomial decomposition a_{ij} may be obtained by minimizing Lagrangian of the system L:

$$L = E_c - E_p^T + W \tag{2}$$

with E_c and E_p^T being, respectively, the kinetic and total potential energies of the system. The term W represents the contribution of (or the work done by) surface loads or body forces. The total potential energy can be written as

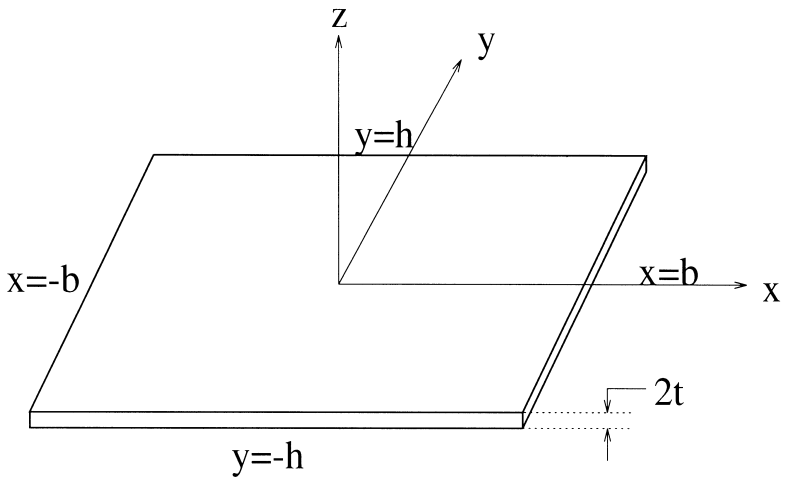

Fig. 2. A thin plate used as the main structure.

$$E_p^T = E_p + E_p^b + E_p^{cp} \tag{3}$$

where E_p is the total strain energy of the main structure, E_p^b is the potential energy stored at the boundary springs and E_p^{cp} is the substructure contribution to the total energy of the coupled system. All terms appearing in the previous equation can be easily determined except for the term E_p^{cp} with

$$E_p^{cp} = \frac{1}{2}\int_{-b}^{b} F_{m'}(x, y_0) D_{m'}(x, y_0)\mathrm{d}x \tag{4}$$

where $F_{m'}(x)$ and $D_{m'}(\xi)$ denote the functions representing the coupling load (force or moment) and the corresponding deformation variations (displacement or rotation), respectively, along the junction. Relation between the two terms can be established using the compliance function $\beta_{m'm'}(x, \xi)$

$$D_{m'}(x, y_0) = \int_{-b}^{b} \beta_{m'm'}(x, \xi, y_0) F_{m'}(\xi, y_0)\mathrm{d}\xi \tag{5}$$

In the above expression, the junction is obviously assumed to be parallel to the x axis with y_0 as its y coordinate. In this same expression (5), the load distribution $F_{m'}(\xi, y_0)$ is an unknown function which constitutes the major obstacle when using the compliance matrix. To tackle this problem, the load distribution along the junction is decomposed over a polynomial base as follows:

$$F_{m'}(\xi, y_0) = \sum_{i}^{m}\sum_{j}^{n} b_{ij}\left(\frac{\xi}{b}\right)^i \left(\frac{y_0}{h}\right)^j \tag{6}$$

with b_{ij} being unknown coefficients to be determined.

The polynomial decomposition for transverse displacements of a rectangular thin plate given by Eq. 1 may be written in a more general form for $D_{m'}(x, y)$ as follows:

$$D_{m'}(x, y) = \sum_{i=0}^{m}\sum_{j=0}^{n} B_{ij}\left(\frac{x}{b}\right)^i \left(\frac{y}{h}\right)^j \tag{7}$$

This equation becomes the same in the case of displacement with $a_{ij} = B_{ij}$.

A regression analysis over the compliance matrix is then to be conducted, giving:

$$B_{m'm'}(x, \xi, y_0) = \sum_{k=0}^{n1}\sum_{l=0}^{n2} c_{kl}^{m'm'} x^k \xi^l \tag{8}$$

An analytical development allows one to find the relation between these two series of coefficients B_{ij} and b_{ij} [1]. Then the energy approach (Rayleigh–Ritz method) allows one to obtain standard second order system with the following energy terms:

$$E_c = \frac{1}{2}\sum_p\sum_q\sum_r\sum_s M_{pqrs}\dot{a}_{pq}(t)\dot{a}_{rs}(t) \tag{9}$$

$$E_p + E_p^b + E_p^{cp} = \frac{1}{2}\sum_p\sum_q\sum_r\sum_s K_{pqrs}a_{pq}(t)a_{rs}(t) \tag{10}$$

where M_{pqrs} and K_{pqrs} are the general mass and stiffness of the system, respectively.

3. Numerical applications

Numerical examples of plate-like structures and beam-stiffened plates are given. The substructures are analyzed analytically or semi-analytically to derive their compliance variations along the contact lines. If desired, analytically derived compliances may be simply replaced by numerical or experimental measurements without any required changes in the formulation. In all forthcoming examples, the components of the coupled system are made of aluminum with modulus of elasticity $E = 0.7E + 11$, mass density $\rho = 2700\frac{kg}{m^3}$ and Poisson's ratio $\nu = 0.3$. A damping factor $\xi = 0.01$ is used in all cases. The main plate is 30 cm wide (2b), 45 cm long (2h) and 3.175 mm thick (2t). These dimensions are kept constant to compare the results obtained for different configurations. In most cases, nine observation points are considered with $n1 = n2 = 8$, where '$n1$' and '$n2$' are the degree of regression for the two independent variables respectively. Any changes in the above mentioned configurations and properties will be specified along the text.

3.1. L-shaped plate

Fig. 3 shows a horizontal plate as the main structure. A vertical auxiliary plate is connected to the main plate. The plates are simply supported along their edges and, consequently, only a rotational moment distribution along the junction is present. This moment distribution is related to the displacement field of the coupled system using the substructure rotational compliance. In all the examples that use L-shaped plates, a transverse force excitation of 100 N is applied at point $x = y = 7.5$ cm of the main plate and the transversal response is measured at the same point.

Fig. 4 shows the response of the L-shaped plate when the auxiliary plate has identical dimensions to the main plate. The response is presented in terms of displacement amplitude and it is compared to the one of a single plate without coupling. Results show that the coupled system has a higher modal density and a slightly lower vibrational level than the single plate (main structure). All original natural frequencies of the main plate, before coupling, are still present in the response of the coupled system. New modes close to these resonances are created. In fact, in most cases, there exists one pair of resonant frequencies which are very close to each other. The first one denotes the resonance of the main and auxiliary plates when vibrating independently. It is due to the fact that identical dimensions are used

for the main and auxiliary plates. This phenomenon of mode splitting is well known in periodically supported structures, which is basically the case here since the main plate and the secondary plate are of identical dimensions. Fig. 5a shows the third mode shape of the coupled system. The main plate seems to be simply supported along the junction and no resistance is imposed from the side of the auxiliary plate. The forth mode of vibration is however quite different. As shown in Fig. 5b, the influence of the substructure is significant and the main plate seems to be closer to a clamped condition along the junction.

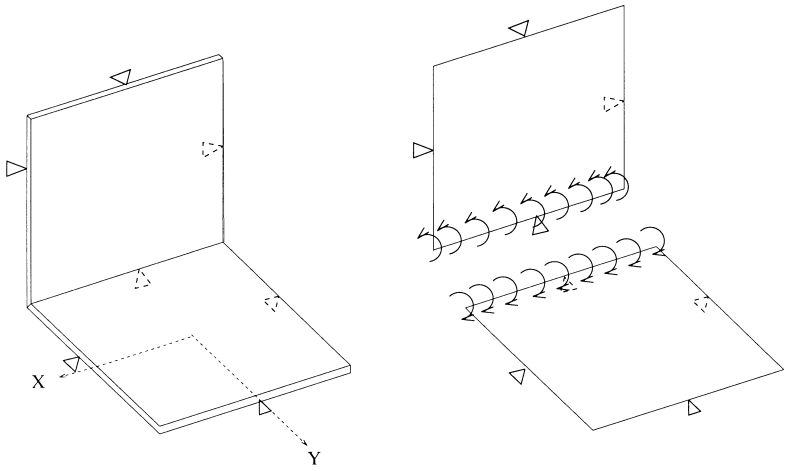

Fig. 3. L-shaped plate, simply supported at the edges.

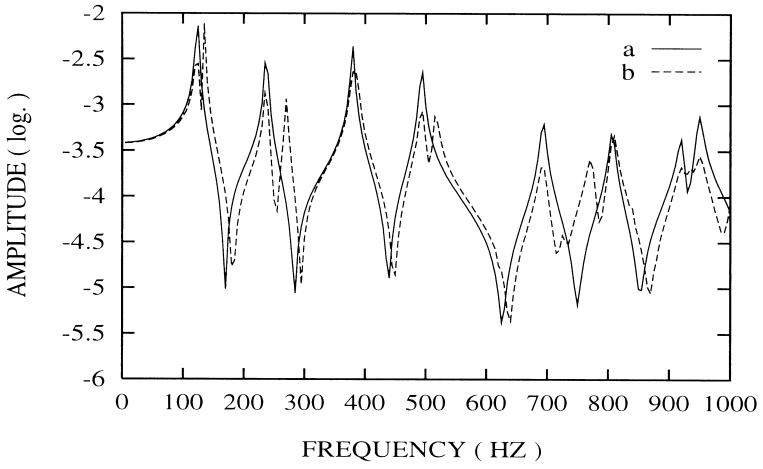

Fig. 4. Response of an L-shaped plate using the CLD technique: (a) response of the main plate before coupling; (b) response of the coupled system.

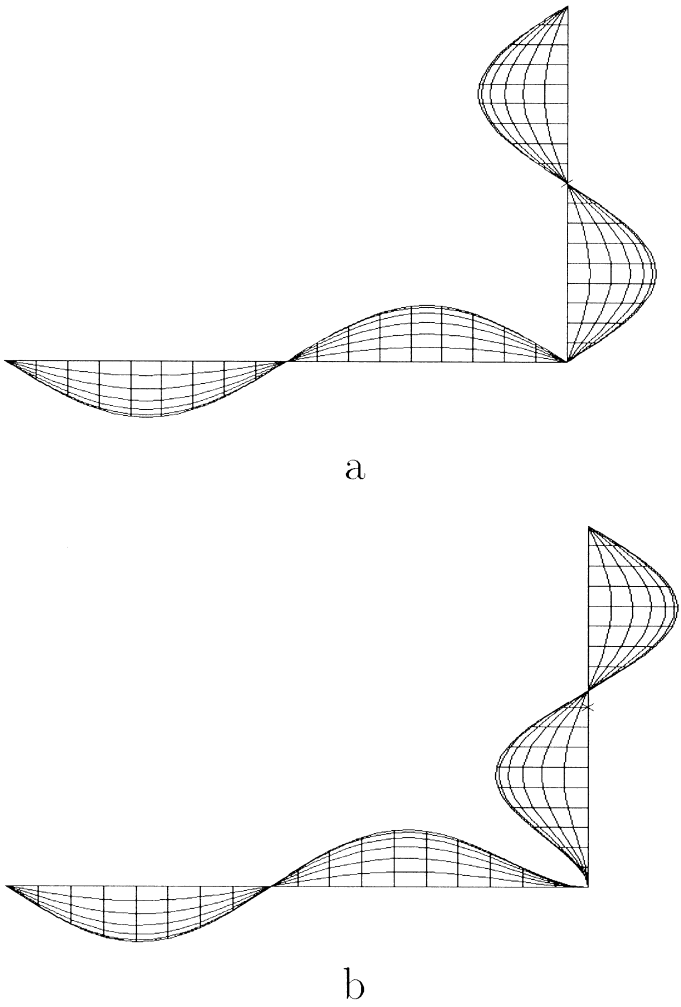

Fig. 5. Mode shapes of the L-shaped plate: (a) third mode (236 Hz); (b) fourth mode (267 Hz).

A finite element simulation using the IDEAS package was conducted in Ref. [1] to validate the CLD technique. Good agreement was observed between the CLD technique and the finite element method using 24 modes over the frequency band of interest of 0–1000 Hz.

The choice of the appropriate number of observation points plays an important role in determining the accuracy of CLD approach. Many methods such as finite element, boundary element and finite difference using spatial or time discretization face the same problem of determining an optimum time or space interval. Generally speaking, the dimensions of the spatial elements must be sufficiently smaller than the wavelength of the structure. It is also the case for the number of contact points between line-coupled structures in the proposed approach. For complex structures

however, it is not always easy to predict the wavelength of the structures as a function of frequency. Sometimes, a rough wavelength estimate may be made by using the wavelength of similar but simpler structures.

Once the wavelength of the substructure is estimated, an appropriate distance between the contact points can be approximately determined. During our simulations, it was noted that the discretization distance should be at least 4 or 5 times smaller than the minimum wavelength in the frequency range of interest. This ensured an acceptable representation of the compliance variation along the junction. The same criteria is used in finite element analysis to estimate a sufficient number of elements for modal analysis of structures.

To illustrate this criteria, let us consider again the simply supported L-shaped plate used previously. The wavelength of the simply supported auxiliary plate is approximated by the wavelength of an infinite plate with the same thickness and material properties. The wavelength of an infinite plate λ is given by the following relation [8]

$$\lambda = \frac{2\pi}{\sqrt{\omega}} \left(\frac{Eh^3}{12\hat{m}(1-\nu^2)} \right)^{\frac{1}{4}} \tag{11}$$

where ω is the radian frequency; E, the modulus of elasticity; $\hat{m}$, the mass per unit area of the plate and ν, the Poisson ratio. Fig. 6 shows the variation of $\lambda/4$ as a function of frequency. In the same figure, the variation of contact point distance Δ is illustrated as a function of the number of contact points using the following relation

$$\Delta = \frac{L}{n-1} \tag{12}$$

where L is the length of the line of contact and n denotes the number of contact points along the same line. Based on those two graphs, one may estimate the

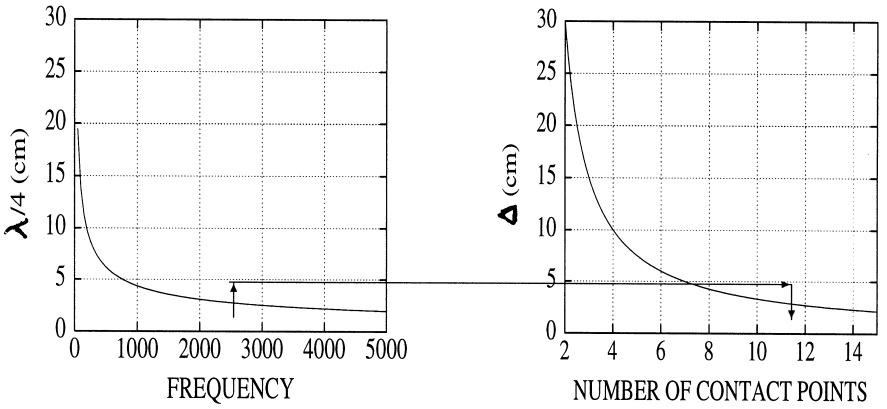

Fig. 6. A simple example to determine the number of contact points required for a plate-like structure.

required number of contact points to analyze the coupled system in a frequency range of interest. For example, to analyze the L-shaped plate up to a frequency of 2500 HZ, one may use 12 contact points. Results using six, eight and nine contact points are compared in Fig. 7. It can be observed that six points are sufficient only up to 600 Hz, while eight or nine points are required to cover the whole frequency range considered. These observations are consistent with the criteria provided above.

3.2. T-shaped plate

Fig. 8 shows two different configurations of T-shaped plates. In the first configuration, the main plate is simply supported at all its edges and at a constraint line along the line $y = 0$ which is also the junction with the auxiliary simply supported plate. The constraint line of the main plate which forms the junction, is supposed to be simply supported. The effect of this constraint line can be easily implemented in the energy equation of the plate in the same way as the contribution of the boundaries, as previously explained. The compliance function of the auxiliary plate along its junction with the main plate must be used to introduce its effect on the main plate.

The second configuration, shown in Fig. 8b, illustrates the case in which the constraint line is placed on the auxiliary plate. In this case, the same steps as for the L-shaped plate must be followed. The compliance function should be obtained for a simply supported plate with an additional simply supported line along its junction with the main plate.

Fig. 9 shows the response of the T-shaped plate of Fig. 8a, when the auxiliary plate has the same physical and material properties as the main plate. The result is

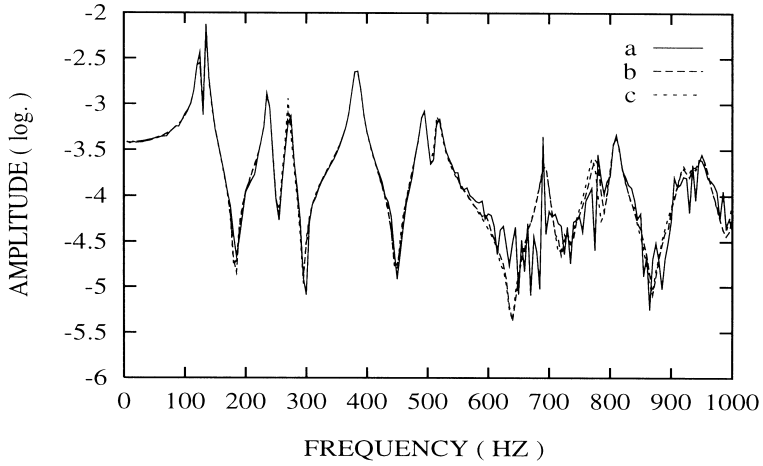

Fig. 7. Response of an L-shaped plate: (a) six contact points; (b) eight contact points; (c) nine contact points.

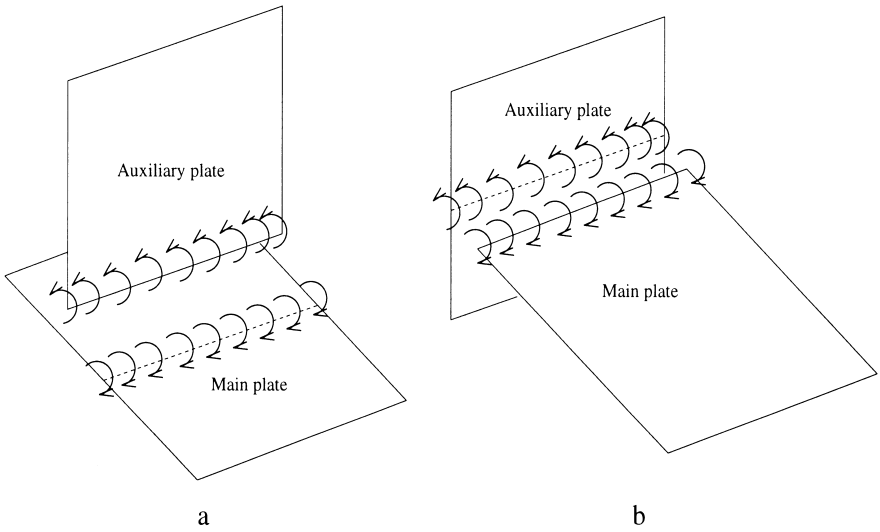

Fig. 8. T-shaped plate: (a) first system; (b) second system.

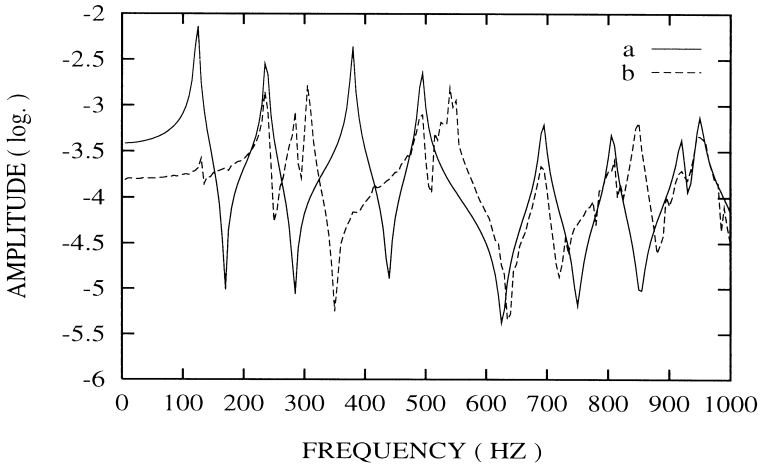

Fig. 9. Response of a T-shaped plate (first configuration): (a) response of the main plate before coupling; (b) response of the coupled system.

compared to the response of the simply supported plate before coupling. As one can observe, the effect of the substructure on the main structure is significant. Vibration level is considerably decreased and the modal density is increased due to the coupling with the auxiliary plate.

In Fig. 10, the response of the coupled system is compared to one obtained by IDEAS. It seems that the CLD method seems to be adequate enough to model the

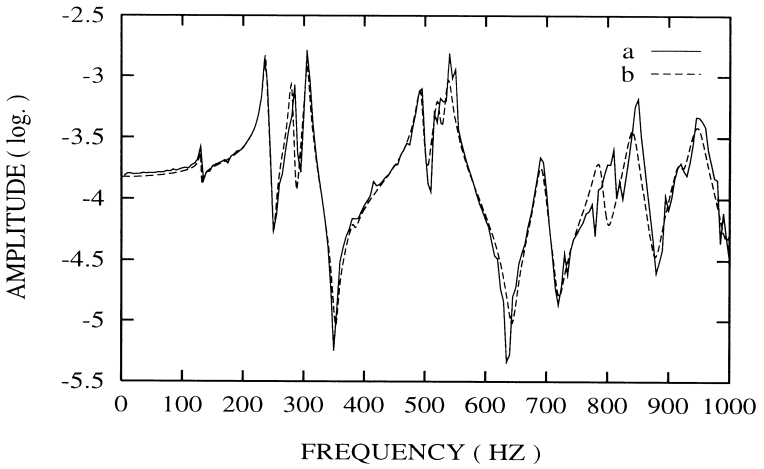

Fig. 10. Response of a T-shaped plate (first configuration): (a) hybrid approach; (b) finite element method.

coupling. The modal analysis using IDEAS shows that there exists 19 modes of vibration up to 1025 Hz while for the main plate, only 10 modes of vibration exist in this frequency range. The fact that all resonances did not appear in the response curve is due to the location of the excitation and response points.

3.3. Ribbed plates with beam stiffeners

As illustrated in Fig. 11, the presence of stiffeners introduces two kinds of coupling with the plate. The first one is related to the torsional effect of the beam which includes a distribution of torsional moment along the junction, and the second one is due to its flexural stiffness, which includes a transverse force distribution. Assuming small deformations, the torsional and flexural behavior of the beam are decoupled and may be treated separately to obtain the compliance matrix.

Consider the plate used in the previous examples as the main structure. As a first step, no eccentricity is considered for the stiffener. This is the configuration that has been widely used in the literature [9]. It means that the neutral axis of the stiffener beam coincide with that of the main plate. From now on, when it is stated that the stiffener has a cross-section of $a \times b$, it means that the stiffener height is b and its width is a (the stiffener is attached to the plate through the a span).

Fig. 12 shows the stiffening effect of the beam on the main plate. The beam has 30 cm in length and is added to the main plate along the line $y = 0$. Compared to the main plate response before coupling, it is observed that all original frequencies of the main plate are shifted toward higher frequencies and at the same time, the vibration level is more or less decreased. The results are also compared with a finite element model. The stiffener is modeled using a linear beam element. The results, shown in Fig. 13, indicate good agreement between both methods.

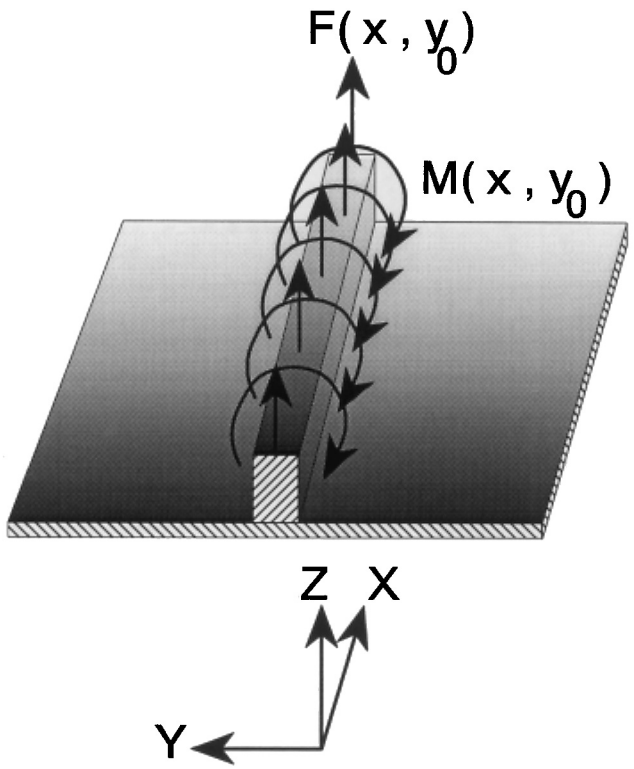

Fig. 11. An example of the beam-stiffened plate.

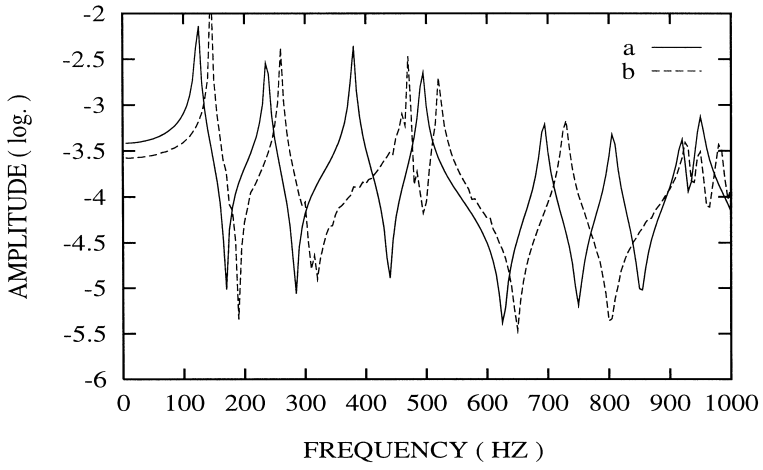

Fig. 12. Response of a beam-stiffened plate: (a) response of a non-stiffened plate; (b) response of the coupled system.

3.3.1. Eccentric stiffeners

In previous examples of beam-stiffened plates, the stiffeners were assumed to be attached to the plate without any eccentricity. In practice, there are many applications in which the stiffener is attached to one side of the plate. Some authors [10–12] have considered the middle line of the plate as the neutral axis of the stiffener, declaring that it is an over estimation of the stiffening effect of the beam.

In the present investigation, a different technique is used to find the neutral axis of the beam in flexural vibration. Fig. 14 shows the cross section of an eccentric beam-stiffened plate. The second moment of inertia of the beam about its middle axis is

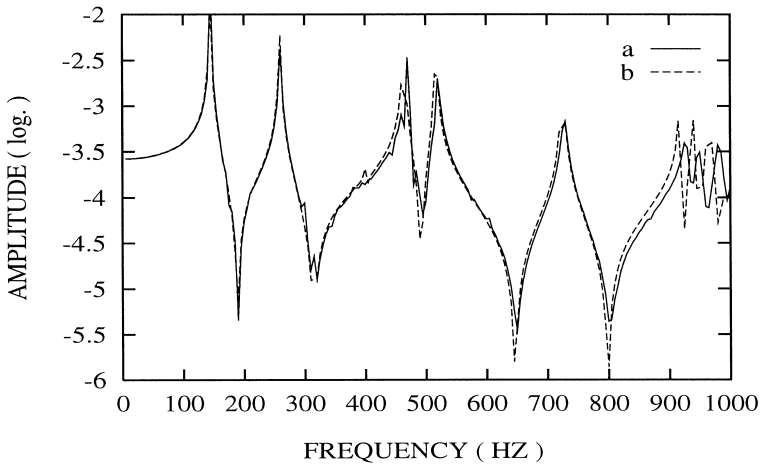

Fig. 13. Response of a beam-stiffened plate: (a) CLD technique; (b) finite element method.

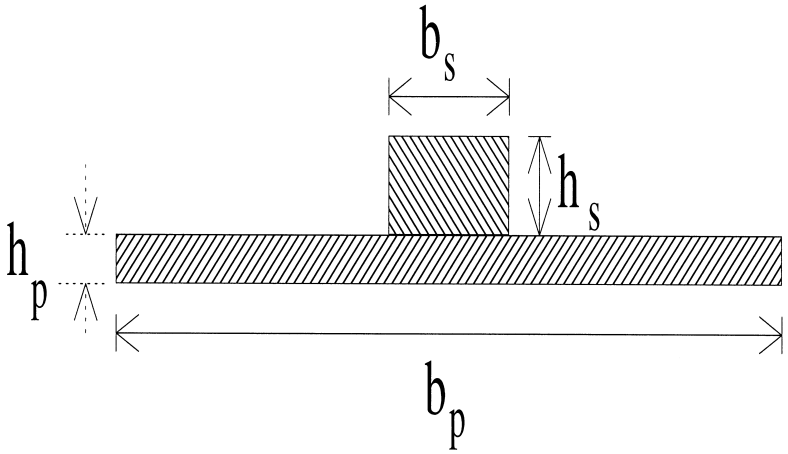

Fig. 14. The cross-section of an eccentric beam-stiffened plate.

$$I_0 = \frac{1}{12} b_s h_s^3 \tag{13}$$

where h_s and b_s are, respectively, the thickness and the span of the beam. The new centroid of the beam (distance from the middle surface of the plate) and modified second moment of inertia of the beam about this new axis are

$$d = \frac{\bar{n} b_s h_s \left(\frac{h_s}{2} + \frac{h_p}{2} \right)}{b_p h_p + \bar{n} b_s h_s} \tag{14}$$

$$I_s = I_0 + b_s h_s \left(\frac{h_s}{2} + \frac{h_p}{2} - d \right)^2 \tag{15}$$

where $\bar{n} = \frac{E_s}{E_p}$, E_s and E_p being the modulus of elasticity of the beam and plate, respectively. The plate thickness is denoted by h_p and its length, along which the beam is coupled, is b_p.

Fig. 15 shows the response of a beam-stiffened plate when the beam of the previous example with cross section 1.5×0.9 cm, is attached to one side of the plate. In the finite element analysis, the elements were the same as those for the case of the beam without eccentricity, but a vertical offset was considered. This vertical offset enables one to model the eccentricity without using the thick plate or brick elements. The torsional constant was not affected by the eccentricity and no modification was made for the torsional properties. Good agreement between the finite element method and the proposed approach was observed.

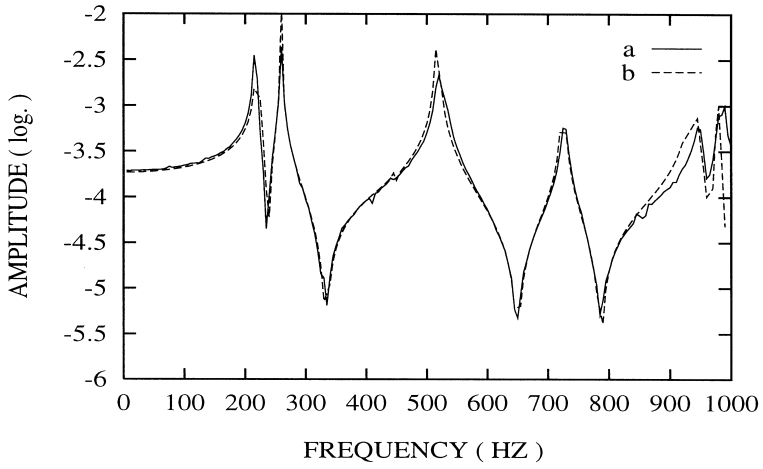

Fig. 15. Response of a beam-stiffened plate with an eccentricity: (a) CLD technique; (b) finite element model.

3.4. Periodic structures and systems with repeated substructures

The subject of periodic structures is a common problem in many applications such as aerospace, ship building and civil engineering. This type of structure may be used to attenuate the wave propagation in solids or to control the vibration level of a system without significantly increasing its mass.

In this section, the efficiency of the CLD method for analyzing coupled systems with repeated substructures is investigated. The advantage of the CLD technique stands in the amount of computational work required which is reduced by a repeated use of the model developed for one of the periodic elements. In this approach, the generalized stiffness matrix of a substructure may be obtained as a function of the global coordinates of the connection line and, therefore, very little effort is required to simulate the coupling of identical elements at different points. When the number of contact points and the degree of regression for different substructures remain unchanged, the dynamic stiffness matrix related to a series of identical substructures can be simply obtained.

This process may be easily repeated for each series of identical substructures. The coupled system can be efficiently treated without repeating previous steps, which are relatively time-consuming procedures, such as measuring or calculating the compliance matrix and performing the regression analysis. The method becomes more appealing when the number of identical substructures increases.

This was assessed using examples of plate assemblies. The previously treated L-shaped plate composed of two identical perpendicular plates is here extended to the case of periodic systems. As a first example, another identical plate is added to the other end of the horizontal plate to form a U-shaped plate. All plates are supposed to be simply supported along the edges. Fig. 16 shows the response of the U-shaped plate compared to the one obtained by a finite element model. For the finite element analysis, the number of nodes and elements used for each plate is identical to the

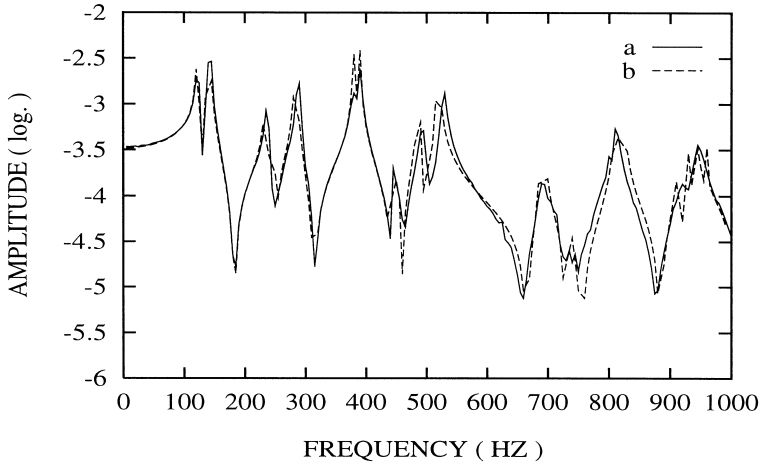

Fig. 16. Response of a U-shaped plate: (a) CLD technique; (b) finite element model.

L-shaped problem treated earlier. The first 25 modes of vibration are superimposed to obtain the forced response of the coupled system. The excitation and response points are the same as those described in the L-shaped plate problem. Generally speaking, Fig. 16 shows good agreement between both methods and, therefore, the CLD technique is capable of representing the general behavior of the plate. It should be mentioned that many factors interfere when one wants to compare the results obtained by these two different methods. The number of elements and the number of eigenfunctions used for mode superposition are important factors in the case of the finite element model. In the case of the CLD technique, the number of contact points, the degree of regression analysis, the number of terms at which the polynomial series of the displacement field and interactive loads are truncated are important parameters which affect the results.

Fig. 17 shows the response of the coupled system when one, two and three identical plates are added to the main structure to form the L-shaped, U-shaped and W-shaped plate, respectively. The third plate is added along the line $Y = Y_0^3 = 0$ which is simply supported as the other edges are. Due to this new supporting line, the vibration level of the coupled system is significantly decreased. The modal density of the coupled system also increases with the number of substructures. For a simply supported plate without any substructure, there exists 10 vibration modes up to 1000 Hz, while this number reaches 18, 22 and 38 when one, two or three vertical plates were added, respectively.

A processing time analysis was performed to study the rate of increase in processing time in the case of a plate like structure. The processing time reference is the U-shaped plate previously treated. Results are shown in Fig. 18 in which computation time increase in percentage is plotted versus the number of sub-structures. In this analysis, the forced responses of all systems are obtained up to 1000 HZ. The polynomial function representing the plate deformation is truncated at $m = n = 10$ for

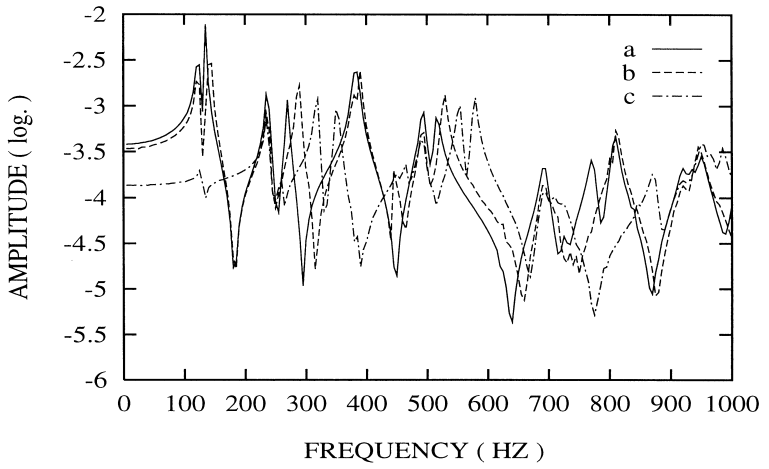

Fig. 17. Comparison between plate-like structures: (a) L-shaped plate; (b) U-shaped plate; (c) W-shaped plate.

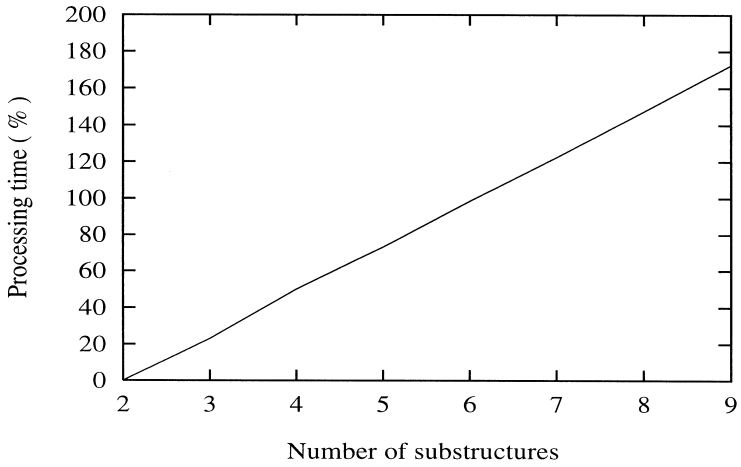

Fig. 18. Rate of increase of processing time with the number of substructures for a plate-like system, using the CLD technique.

all coupled systems. Fig. 18 shows that the addition of substructures does not significantly increase processing time. There is an increase of 40% in processing time when two other plates are added to the original configuration. Adding six plates to the original configuration leads to only 140% increase in processing time.

4. Conclusions

Vibrations of typical coupled structures along a continuous line were investigated using the CLD technique. Numerical examples of the plate-like structures and beam-stiffened plates were given. These examples were chosen such that cases of weak and strong influences were studied. Results obtained were compared to finite element models and good agreement was observed. It can be seen the CLD technique is capable of dealing with a large variety of mechanical structures coupled through a continuous line. Using the criteria established in the present paper, reasonably good results can be obtained by properly choosing observation points for compliance calculation or measurement. It was also shown that the method is efficient to analyze periodic structures and systems with repeated substructures. Further investigations are still needed to extend the applications of CLD technique to more complex cases. Curved periodically ribbed panel is a typical example.

References

[1] Hatam M, Cheng L, Rancourt D. Vibration analysis of line-coupled structures using a coupling load decomposition technique. The Journal of Acoustical Society of America 1998;103(6):3376–85.
[2] Lyon RH. Statistical energy analysis of dynamical systems, theory and applications. Cambridge (MA): MIT Press, 1975.

[3] Soize C. A model and numerical method in the medium frequency range for vibroacoustic predictions using the theory of structural fuzzy. The Journal of Acoustical Society of America 1993;94:849–65.
[4] Goyder HGD, White RG. Vibrational power flow from machines into built up structures, part 1: introduction and approximate analysis of beam and plate-like foundations. Journal of Sound and Vibrations 1980;68(1):59–75.
[5] Hurty WC. Dynamic analysis of structural systems using component modes. AIAA Journal 1965;3(4):678–85.
[6] Suarez LE, Singh MP. Modal synthesis method for general dynamic systems. Journal of Engineering Mechanics 1992;118(7):1488–503.
[7] Gladwell GML. Branch mode analysis of vibrating systems. Journal of Sound and Vibrations 1964;1:41–59.
[8] Cremer L, Heckl M, Ungar EE. Structure-borne sound. Springer-Verlag (chapter V, section 5).
[9] Dowell EH. Free vibrations of an arbitrary structure in terms of component modes. Journal of Applied Mechanics 1972;39:727–32.
[10] Kirk CL. Natural frequencies of stiffened rectangular plates. Journal of Sound and Vibration 1970;13(4):375–88.
[11] Goldfracht E, Rosenhouse G. Use of Lagrange multipliers with polynomial series for dynamic analysis of constrained plates part I: polynomial series. Journal of Sound and Vibration 1984;92(1):83–93.
[12] Rosenhouse G, Goldfracht E. Use of Lagrange multipliers with polynomial series for dynamic analysis of constrained plates, part II: Lagrange multipliers. Journal of Sound and Vibration 1984;92(1):95–106.